ADVANCED MATERIALS INTERFACES
www.advmatinterfaces.de

Rub-Resistant Antibacterial Surface Conversion Layer on Stainless Steel

Haiyue Huang, Olivia Willilams Barber, Zhilong Yu, Hun Park, Xiaobing Hu, Xinqi Chen, Chun-Hu Chen, Erica M. Hartmann, and Jiaxing Huang**

Stainless steels are widely used in hospitals and public transportation vehicles as one of the most common touch surfaces. Retrofitting stainless steel surfaces with an antimicrobial layer can bring potential public health benefits by reducing the ability of inanimate objects, or fomites, to transmit infections. Here, a facile surface conversion reaction between stainless steel and a solution of $KMnO_4$ and $CuSO_4$ is reported, which leads to a conformal and robust oxyhydroxide layer. Microscopy observations show that the layer is amorphous, continuous, and pinhole-free with a thickness of only 10–15 nm. The coating adheres strongly to stainless steel and can resist rubbing in simulated friction tests, which is attributed to its intermixing with the substrate without forming a sharp interface. Cu ions incorporated into the surface layer can be released into water droplets deposited on the surface and induce antimicrobial activities against bacteria (*Pseudomonas aeruginosa* PA14) after 30 min of contact.

1. Introduction

Cu is a broad-spectrum antimicrobial agent utilized in various forms and valences such as metallic Cu, alloy, oxide, and ion.[1] Coatings consisting of Cu, especially those grown on frequently touched surfaces, are important tools to reduce fomite infections and improve public health.[2] In many hospitals and throughout public transportation systems, stainless steel is one of the most common materials due to its resistance to corrosion, appropriate mechanical properties, and processability. However, stainless steel does not have antimicrobial properties. An ideal disinfecting coating on stainless steels should be durable, safe, and easy to grow. These criteria, however, are challenging to be met simultaneously. For example, a high temperature and/or a high level of vacuum are often required to grow metallic Cu or its alloy on stainless steels, such as plasma spray, wire arc spray, and chemical vapor deposition.[3] Paintings of metallic Cu and Cu oxides particles composited with polymers may suffer from poor adhesion on the substrate, especially when considering the curved shape and fine finish of stainless steel used in those scenarios. Cu ions have also been investigated in coating techniques, such as those using zeolite,[4] laponite,[5] and polyanion[6] as the anchoring agents. Pre-loaded Cu ions can be released into the local aqueous environment of microorganisms to cause inactivation. However, these methods are currently limited to specific types of substrates and are not applicable to stainless steel.

The challenge of growing an adherent coating on stainless steel is attributed to its chemical inertness. One way to overcome this is through surface reactions based on a strong oxidizing agent, such as $KMnO_4$. This has been utilized for in situ synthesis of electrocatalyst, as reported by previous studies.[7] The reaction between $KMnO_4$ based precursor solution and stainless steel is spontaneous and self-limiting, leaving a thin and conformal oxyhydroxide surface layer. By adding Cu salts into the precursor solution, we developed a simple method to obtain a Cu-containing coating. It was found that Cu ions can leach from the coating, which may have caused the improved antibacterial activity compared to bare substrates. This solution-processing method can be applied to retrofit already-installed stainless steel parts, such as doorknobs and elevator buttons, with a conformal yet strongly adhering nanocoating for improved antibacterial properties.

H. Huang, Z. Yu, H. Park, X. Hu, J. Huang
Department of Materials Science and Engineering
Northwestern University
Evanston, IL 60208, USA
E-mail: jiaxing-huang@northwestern.edu
O. W. Barber, E. M. Hartmann
Department of Civil and Environmental Engineering
Northwestern University
Evanston, IL 60208, USA
E-mail: erica.hartmann@northwestern.edu
X. Hu, X. Chen
The NUANCE Center
Northwestern University
Evanston, IL 60208, USA
X. Chen
Department of Mechanical Engineering
Northwestern University
Evanston, IL 60208, USA
C.-H. Chen
Department of Chemistry
National Sun Yat-sen University
Kaohsiung 80424, Taiwan

The ORCID identification number(s) for the author(s) of this article can be found under https://doi.org/10.1002/admi.202200251.

DOI: 10.1002/admi.202200251

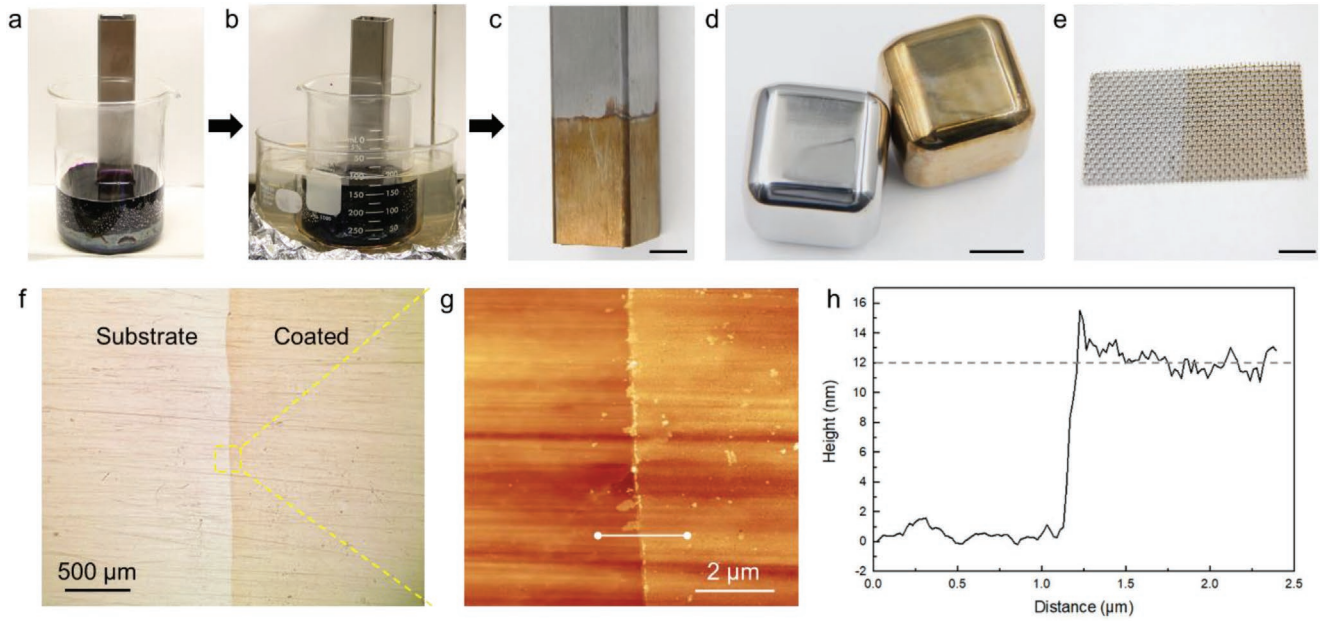

Figure 1. Coating stainless steel with a dense and conformal thin layer through surface reaction. a) A stainless-steel bar is immersed in an aqueous mixture of $CuSO_4$ and $KMnO_4$, and b) heated at 85 °C for 1 h. c) After rinsing in water and ethanol, the substrate is coated with a gold/brown colored layer. Same procedures can be applied to objects with various geometries such as d) a cube and e) a mesh made of stainless steel. f) Optical microscopy image and g) AFM image showing the coating is uniform and continuous. h) The line profile extracted from (g) indicates a thickness of 10–15 nm. Scale bars in c–e) are 1 cm.

2. Results and Discussion

2.1. Preparation and Characterization of the Surface Layer

The preparation of the Cu-containing surface layer was carried out by simply dipping stainless steels into precursor solutions at 85 °C for 1 h. The precursor solution contains different ratios of $CuSO_4$ and $KMnO_4$ dissolved in deionized (DI) water. For reasons that will be discussed later, a molar ratio of 3:1 was used for most of the experiments. A gold/brown layer was grown on the immersed part of the substrate, as can be seen in **Figure 1**a–c. This method is applicable to objects of different shapes and surfaces with different curvatures, such as a cube and a mesh (Figure 1d,e). The coating was continuous and uniform in color under an optical microscope (Figure 1f). It was pinhole free with a thickness of only around 10–15 nm, as demonstrated in Figure 1g by observation under an atomic force microscope (AFM). The formation of a conformal coating implies that this strategy could be used in combination with surface patterning, such as nanotexturing,[8] to have synergistic and enhanced antimicrobial effects.

X-ray photoelectron spectroscopy (XPS) shows the elements of the surface layer including Mn, Cu, Fe, and O. To reveal the underlying composition, depth profiling for Cu, Mn, and Fe signals was conducted with their results shown in **Figure 2**a–c. For Cu, the spectrum at the surface has two signals at 954.3 ($Cu2p_{1/2}$) and 934.4 eV ($Cu2p_{3/2}$) with strong satellite peaks, indicating the presence of Cu(II). After one etch cycle, Cu(II) signal is replaced by Cu(I) signal characterized by two peaks at 953.0 and 933.2 eV. This turns out to be an artifact caused by argon ion sputtering during etching.[9] Control experiments conducted on a mechanically scratched coating as well as on the cross section both detected only Cu(II) instead of Cu(I) in the XPS spectra (Figure S1). The oxidation state of Mn could be Mn(III) or Mn(IV) as the Mn2p spectra with two peaks at 653.7 and 642.1 eV are not sufficient to distinguish the two. For a similar reason as Cu, the oxidation state of Fe in the thin film is most likely Fe(III) instead of Fe(II). Going deeper into the substrate, oxidized Fe is gradually replaced by metallic Fe. As for the O spectrum (Figure S2, Supporting Information), it consists of both hydroxide and O^{2-} peaks, indicating it is a multi-component metal oxyhydroxide film.[10]

The depth profiles of Cu, Mn, O, and Fe in the coating are plotted in Figure 2d. The atomic ratios of Cu, Mn, and O generally decrease, while that of Fe increases as the etching time increases. The coating can be divided into three zones along the depth, namely the surface layer, the interdiffusion zone, and the substrate. Starting from the outer surface, the transitions between these three zones are characterized by the crossover points of Cu and Fe profiles and Fe and O profiles. This gradual change of relative concentration of each element is illustrated in Figure 2e, which resembles the typical microstructure of passive films grown on stainless steel.[11] The presence of Fe above the substrate zone indicates that the deposition of the oxyhydroxide coating is accompanied by corrosion of stainless steel. There are no sharp interfaces between these three zones, suggesting strong adhesion of the coating.

The valence of Cu in the coating layer is unchanged from that in the precursor solution, which implies that the incorporation of Cu does not include redox reactions and is most likely a co-precipitation process. As $KMnO_4$ oxidizes Fe, Mn(III or IV) and Fe(III) oxyhydroxide starts to form, the deposition of which fixes Cu(II) as part of the structure, probably through oxygen-bridged bonding.[12]

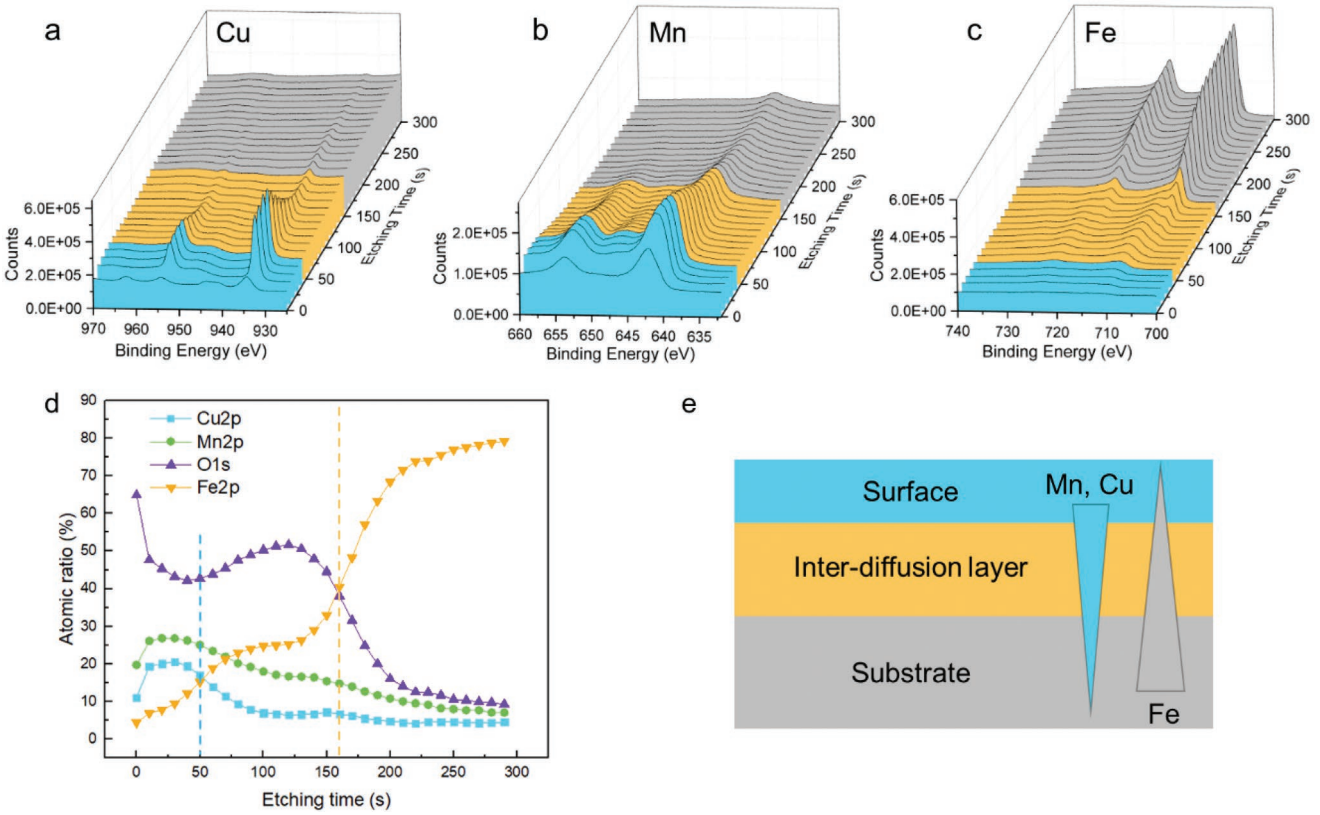

Figure 2. X-ray photoelectron spectroscopy (XPS) analysis of the coating. a–c) Sets of spectra corresponding to Cu, Mn, and Fe measured during XPS depth profiling. d) Atomic ratios of the main elements in the coating as a function of etching time (i.e., depth into the film). e) Schematic illustration of the three zones along the thickness of the coating, including the Cu-rich surface (blue), an interdiffusion zone (yellow), and the substrate (grey). The blue and grey triangles indicate the change of the Mn/Cu and Fe content across the interface.

The microstructure of this oxyhydroxide layer is characterized by transmission electron microscopy (TEM) with high spatial resolution. **Figure 3**a shows a bright field (BF) cross-sectional view image obtained in scanning TEM (STEM) mode, which is used as a reference for energy dispersive X-ray (EDX) mapping. Figure 3b–d demonstrate the distributions of Fe, O, and Mn along the thickness of the coating. Considering that some scattered electrons at high angles will strike other Cu-containing TEM parts (e.g., sample holder, polepiece), the Cu signal is not deemed reliable and thus not shown here. Elemental maps of Mn and O show their distribution across the zones, which is consistent with the XPS results. The mapping also shows that the elemental distribution along the horizontal direction is rather uniform. A thickness of around 10 nm determined from the cross-sectional view in Figure 3e agrees with the previous AFM result (see Figure 1h). Fast Fourier transform (FFT) patterns (Figure 3f) taken from several regions indicate the coating is amorphous.

2.2. Total and Leachable Content of Cu Ions

It was found that Cu ions in the surface layer can be released upon in contact with water, which is useful for antimicrobial activities because pathogen-containing particulates can often hold capillary condensed moisture.[2a,13] To optimize the total and leachable content of Cu ions, coatings were prepared from different ratios of $CuSO_4$ to $KMnO_4$ in the precursor solutions with a constant $KMnO_4$ concentration. Coated stainless steels were then soaked in DI water to allow leaching of Cu ions, the concentration of which was measured by inductively coupled plasma mass spectrometry (ICP-MS) and plotted against time up to 500 min (**Figure 4**a). Coatings prepared from the precursor of an atomic ratio of 3:1 ($CuSO_4$ versus $KMnO_4$) lead to the quickest Cu ion release curve compared to 5:1 and 1:1. The total content of Cu in the coating was estimated by dissolving the coating completely using a strong acid followed by an ICP-MS analysis of the resulting solution. Figure 4b compares the total Cu content of each film as well as that of released into the water after 500 min. It can be seen that 3:1 is the optimal ratio resulting in the highest content of both total and leached Cu. When the ratio was increased to 5:1, the coating became inhomogeneous (see Figure S3, Supporting Information). Therefore, samples made with a 3:1 ratio of $CuSO_4$ to $KMnO_4$ are deemed optimal and thus used for most of the experiments in this work, including the antibacterial tests. In contrast to Cu, no obvious Mn or Fe was detected after soaking the samples in water. This implies Cu ions may be adsorbed or intercalated in a framework mainly made of manganese oxyhydroxide,[14] and they can diffuse out of the coating upon contact with water.[15]

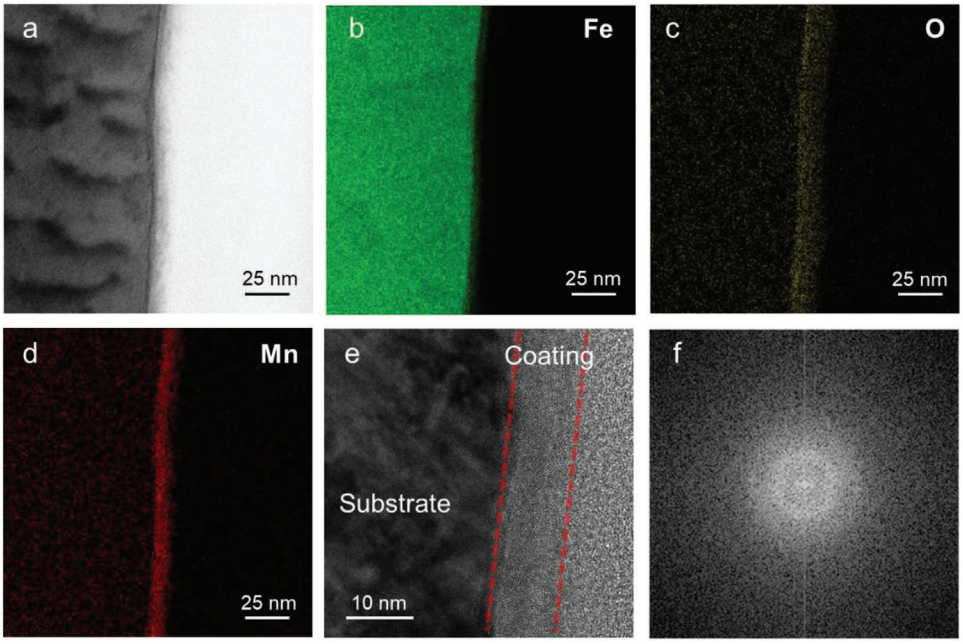

Figure 3. High spatial resolution transmission electron microscopy (TEM) study of the coatings. a) Bright field image obtained in scanning TEM mode (BF-STEM) of the cross-section showing the substrate-coating interface. b–d) EDX mapping in the same area showing distribution of Fe, O, and Mn across the interface. Mapping of Cu is not shown due to artifact signal from environmental objects. e) High-resolution TEM (HRTEM) image of the coating. f) Corresponding FFT pattern showing the nearly amorphous nature of the coating.

2.3. Durability of the Surface Layer

Durability is an important feature for coatings on touch surfaces. Considering the small thickness of the oxyhydroxide layer and the low temperature used for deposition, the adhesion might have been a concern. However, this coating is rather robust against daily wear and shear in simulated experiments. As shown in **Figure 5**a, a black hard rubber ball was pressed on the surface with a force of 5 N, which was equal to a pressure of 1.1 MPa based on the contact area indicated by the two red dashed lines in Figure 5b. The ball was then rubbed back and forth for 2400 times, which is a more aggressive condition compared to daily wear and shear during touch. Figure 5b shows that debris of the rubber ball was visible after the test due to strong friction and wear. However, after washing away the debris, no obvious wear or damage of the coating in the rubbed area can

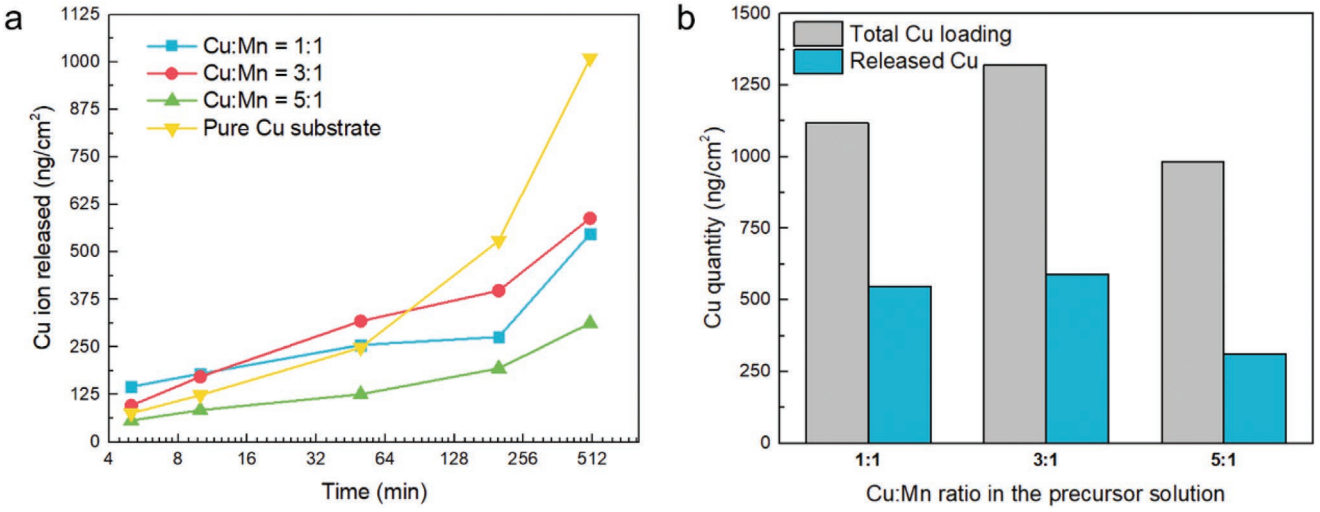

Figure 4. Evaluation of Cu ions leached out from the coating. a) The quantity of Cu ions released from the coated stainless steel into water over time. Coatings prepared with different ratios of $CuSO_4/KMnO_4$ in the reaction are examined and compared with a pure copper foil. b) Total Cu loading in the coatings and the corresponding quantity of released Cu ions after 500 min, for coatings prepared under different ratios of precursors. This helps to determine the optimal formulation for making the coating.

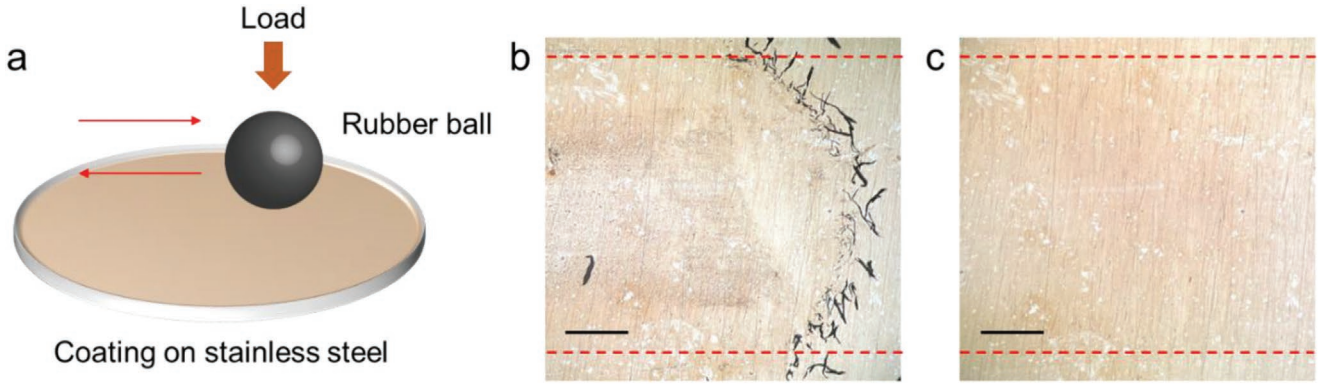

Figure 5. Adhesion and durability test. a) Schematic drawing illustrating the experimental setup for durability test. A hard rubber ball was pressed on the coated substrate with a pressure of about 1.1 MPa and rubbed back and forth for 2400 times. b) Optical microscopy image taken right after the test showing the presence of rubber debris. c) After washing away the rubber debris, no obvious loss of the coating can be observed in the rubbing zone (indicated by two red dashed lines). Scale bars in b) and c) are 500 µm. The durability of the coating can be attributed to the formation of an interdiffusion layer observed in the XPS study (Figure 2).

be observed. The excellent adhesion is attributed to the formation of the interdiffusion zone between the coating and stainless steel (see Figure 2), which minimizes the residual stress.

2.4. Antibacterial Activity

As a proof-of-concept of the antimicrobial functions, susceptibilities of two bacterial strains were evaluated. *Pseudomonas aeruginosa* PA14 and *Staphylococcus aureus* (ATCC25923) were selected to represent Gram-negative and Gram-positive isolates, respectively. For comparison, control samples include uncoated stainless-steel plates and coated samples that had been soaked in DI water at room temperature for 24 h to deplete Cu ions. The as-coated, extensively washed, and uncoated stainless steels were then tested for antibacterial activities (see Experimental Section for details).

Cu ions can lead to the death of bacteria via several mechanisms, including the generation of reactive oxygen species (ROS), membrane damage, and DNA degradation.[1b,d] The results in **Figure 6** show that the coating has significant disinfecting effects for *P. aeruginosa* PA14 but not for *S. aureus*. The difference may be due to the thinner peptidoglycan layer in Gram-negative bacteria, which could make it more susceptible to Cu ions than Gram-positive bacteria.[16] For *P. aeruginosa* PA14, both the as-made coatings and the washed coatings show significantly better antibacterial activities compared to uncoated stainless steels after only 30 min of contact (Table S1, Supporting Information). The as-made coating has a higher log reduction compared to the washed coating, suggesting releasing Cu ions into the aqueous environment plays an important role in decreasing the live bacterial load on the oxyhydroxide layer. The performance of these coatings was also benchmarked against pure Cu plates, which have a significantly higher log reduction (Table S2, Supporting Information). Note that Figure 4 shows the concentration of released Cu ions from the coating is in the same order as pure Cu. As releasing profiles were measured in DI water, the much lower antibacterial activity of coated stainless steels can be attributed to the depletion of Cu ions from the coating, while Cu plates are an unlimited reservoir for Cu ions.

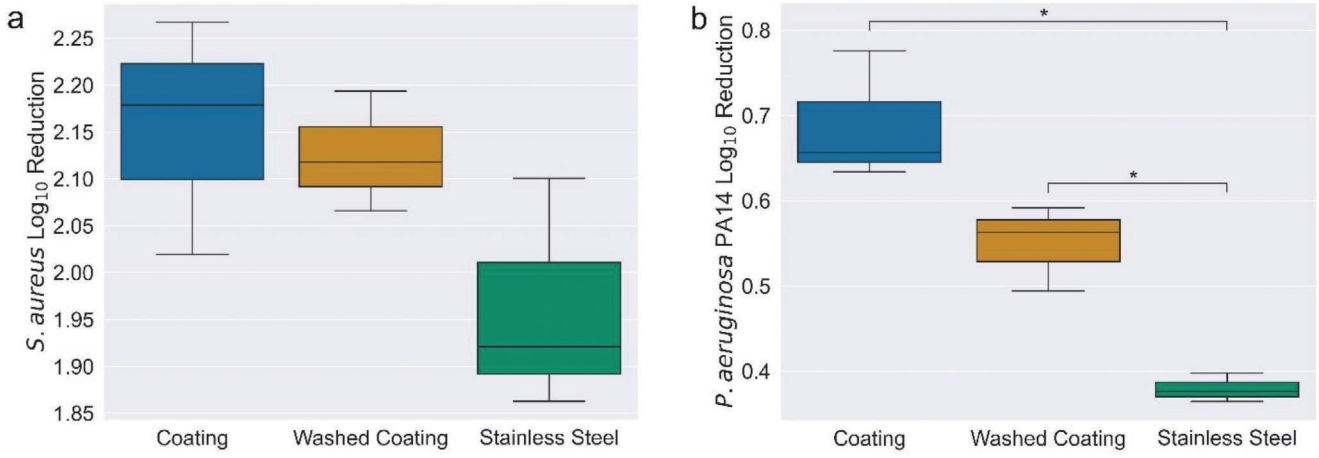

Figure 6. Antibacterial activity. Log_{10} reduction after 30 min for a) *Staphylococcus aureus* and b) *Pseudomonas aeruginosa* PA14 on the as-synthesized coating, washed coating, and bare stainless steels (*$p < 0.05$ from Welch's test). Washed coating was prepared by soaking coated stainless steels in DI water for 24 h to reduce loading of leachable Cu ions.

The coating releases copper ions in the presence of water, which is common around deposited particulate matter due to capillary condensation. The dry transfer would only pick up those copper ions on the atomic surface of the coating. Therefore, hand transfer should be minimal because of the relatively low moisture content on hand and the brief interaction time during common touches. Further work is needed to improve the effectiveness of S. aureus (Gram-positive) bacteria or to find better testing protocols that can best simulate how the coating is used for curbing fomite infection.

3. Conclusion

This work demonstrates an easy one-step surface conversion method for depositing an antimicrobial coating onto stainless steel. The formation of an interdiffusion zone instead of a sharp interface renders the coating excellent durability against friction during touch. Cu ions loaded on the layer can be partially and quickly released into water, which likely contributes to antibacterial activity against *P. aeruginosa* PA14 after 30 min. The current coating is conformal, continuous, and rub-resistant and offers a good foundation for engineering better antimicrobial surfaces on stainless steels. The performance may be further improved by adjusting synthesis parameters to incorporate more Cu, such as by adjusting temperature and precursor anions. Antimicrobial surface is an important method to reduce fomite infections by pathogens, including those that cause respiratory diseases. More studies in the future are needed to evaluate disinfecting effects against other microorganisms such as viruses or fungi.

4. Experimental Section

Preparation of the Surface Layer with Leachable Cu Ions: Stainless steel substrates (type 304, Alfa Aesar, 0.05 mm thick) were first cleaned by soaking in acetone for 5 min to remove organic residuals on the surface. They were then activated by soaking in 0.5 M HCl for another 5 min to remove any possible surface passivation layer. After that, substrates were immersed in a water solution of different ratios of $KMnO_4$ and $CuSO_4$. The concentration of $KMnO_4$ was kept at 0.04 mol L^{-1}. For example, for a ratio of 3:1, 0.04 mol L^{-1} of $KMnO_4$ and 0.12 mol L^{-1} of $CuSO_4$ were mixed in DI water and preheated at 85 °C for 15 min. Substrates were then soaked inside at 85 °C for 1 h, after which coated substrates were removed from the solution bath and purified by soaking and agitating in water for 5 s and then in ethanol for 5 s. Coated substrates had a gold to brown hue.

Characterization: The thickness was measured using AFM (Bruker Dimension FastScan). XPS was conducted on Thermo Scientific ESCALAB 250Xi. The carbon peak for reference was 285.1 eV, no manual adjustment of the chemical shift was made. Argon ion sputtering was set to 2 kV with an area of 2.5 mm^2. Optical microscopy images were taken from Nikon Eclipse E600 POL upright microscope. Electron transparent lamellar samples were prepared using FEI Helios. TEM characterizations were performed on an ARM 200CF microscope operated at 200 keV. This microscope was equipped with the probe corrector and dual silicon drift detectors (SDDs).

Evaluation of Quantity of Cu Ions: Stainless steels were cut into pieces of 20 × 10 mm^2. After being coated, they were soaked in 10 mL of DI water without agitation. After a certain time, water was decanted out and analyzed by ICP-MS (Thermo iCAP Q). It should be noted that for accurate measurement, plastic vials (Falcon tubes, Fisher Scientific) were used instead of glass vials. Pure copper foils (Alfa Aesar, Puratronic, 99.9999%) with a dimension of 13 × 13 mm^2 were immersed in 10 mL of water and were evaluated in the same way. The experiment was repeated three times and a typical curve was shown in the figure. To measure the total loading of Cu on coated stainless steels, samples were soaked in 0.5 M HCl for 12 h. The concentration of Cu ions dissolved in HCl was then evaluated by ICP-MS.

Durability Test: Durability of the coating against rubbing was studied using a tribological tester with a ball-on-disk geometry. The hard rubber ball was purchased from McMaster-Carr. It has a diameter of 3/8″ (9.5 mm) and tensile strength of 2100 psi (14.5 MPa) according to the description from the manufacturer. The coated stainless steel (from a $CuSO_4$ to $KMnO_4$ ratio of 3:1) was then fixed tightly on the holder of the tribometer. The tests were conducted at a linear speed of 80 mm s^{-1} and a frequency of 4 Hz with a constant vertical force of 5 N. Each experiment last 5 min, which equals 2400 times of rubbing.

Antibacterial Activity: Stainless steels were cut into pieces of 20 × 20 mm^2 and coated following the same procedures as described above. To get washed coating, the as-coated films were soaked in 1 L of DI water for 24 h. Films were cleaned using ethanol and then placed into petri dishes to be sterilized under UV light for 30 min. Each individual isolate was grown to the late exponential phase in 10 mL tryptic soy broth (TSB). Cells were then pelleted by centrifugation at 3000 rpm for 5 min and resuspended in 1 mL inoculum saline (Beckman Coulter, Brea, CA). 25 µL of late exponential phase cell saline suspension corresponding to 3.4×10^7 colony forming units (CFUs) for *P. aeruginosa* PA14 and 3.2×10^9 CFUs for *S. aureus* was transferred onto films. They were then transferred to the 37 °C incubator for 30 min and then recovered.

Bacterial Sample Recovery and Dilution: Bacterial samples were collected using wet swabbing with Puritan HydraFlock 6" Sterile Standard Flock Swabs (Puritan, Guilford, ME). The tip of the swab was dipped into a 15 mL tube containing 1 mL of phosphate-buffered saline (PBS). The swab was wiped across the surface left to right, top to bottom, and right to left for 10 seconds in each direction. The swab was then placed into the tube containing 1 mL of PBS. Tubes containing swabs were vortexed for 1 min total at 10 s intervals. Next, the swabs were squeezed against the 15 mL tube to expel the remaining liquid and removed. The samples were then vortexed for 5 s. Ten-fold special dilutions of each sample were created using PBS as the diluent and 10 µL of each dilution was plated on tryptic soy agar (TSA). The plates were then placed in the incubator at 37 °C for 20–24 h. After 20–24 h, the colonies were counted and CFU was determined in the original samples. The least diluted plate able to have the CFU quantified (having between 30 and 300 colonies per plate) was used to estimate the CFU mL^{-1} in the given sample, i.e., if 10^{-4} had 100 CFU after 24 h and 10^{-5} had 20 CFU, 10^{-4} with 100 CFU was used to determine the original sample density. Dilutions of the initial culture were also plated to calculate the original culture CFU.

Statistical Analysis: The Welch's *t*-test was conducted using R (version 4.1.0). Results were considered statistically significantly different with $P < 0.05$.

Supporting Information

Supporting Information is available from the Wiley Online Library or from the author.

Acknowledgements

The work was supported by Office of Naval Research (ONR N000142012685). This work made use of the SPID, Keck-II, and EPIC facility of Northwestern University's NUANCE Center, which had received support from the SHyNE Resource (NSF ECCS-2025633), the IIN, and Northwestern's MRSEC program (NSF DMR-1720139). H.H. thanks the support from Northwestern University through a Ryan Fellowship and a Dissertation Fellowship. O.W.B. was supported in part

by the Biotechnology Training Program. The authors thank Prof. Jane Wang and Dr. Pan He for help with the tribometer, and Po-chun Liao for initial assistance. The authors further thank Dr. Egon Ozer for providing *P. aeruginosa* PA14.

Conflict of Interest

The authors declare no conflict of interest.

Data Availability Statement

The data that support the findings of this study are available from the corresponding author upon reasonable request.

Keywords

antimicrobial coating, oxyhydroxide, stainless steel, surface conversion layer

Received: February 1, 2022
Published online:

[1] a) G. Grass, C. Rensing, M. Solioz, *Appl. Environ. Microb.* **2011**, *77*, 1541; b) M. Vincent, R. E. Duval, P. Hartemann, M. Engels-Deutsch, *J. Appl. Microbiol.* **2018**, *124*, 1032; c) O. Barber, A. Khan, E. M. Hartmann, D. Isheim, S. Vaynman, Q. J. Wang, Y. W. Chung, *Adv. Mater. Process* **2020**, *178*, 25; d) J. A. Lemire, J. J. Harrison, R. J. Turner, *Nat. Rev. Microbiol.* **2013**, *11*, 371; e) J. L. Zhao, D. K. Xu, M. B. Shahzad, Q. Kang, Y. Sun, Z. Q. Sun, S. Y. Zhang, L. Ren, C. G. Yang, K. Yang, *Appl. Surf. Sci.* **2016**, *386*, 371.

[2] a) H. Y. Huang, C. H. Fan, M. Li, H. L. Nie, F. B. Wang, H. Wang, R. Wang, J. B. Xia, X. Zheng, X. L. Zuo, J. X. Huang, *ACS Nano* **2020**, *14*, 3747; b) D. Mitra, E. T. Kang, K. G. Neoh, *Acs Appl Mater Inter* **2020**, *12*, 21159; c) M. Vincent, P. Hartemann, M. Engels-Deutsch, *Int J Hyg Envir Heal* **2016**, *219*, 585.

[3] a) I. A. Hassan, I. P. Parkin, S. P. Nair, C. J. Carmalt, *J. Mater. Chem. B* **2014**, *2*, 2855; b) V. M. Villapun, L. G. Dover, A. Cross, S. Gonzalez, *Materials* **2016**, 9, 736.

[4] K. Imai, H. Ogawa, V. N. Bui, H. Inoue, J. Fukuda, M. Ohba, Y. Yamamoto, K. Nakamura, *Antivir Res* **2012**, *93*, 225.

[5] X. M. Tang, J. Dai, H. L. Sun, N. Saha, P. Saha, L. C. Tang, Q. L. Cheng, D. Q. Wang, J. Wei, *J. Nanomater.* **2018**, *2018*, 5470814.

[6] P. F. Li, Z. C. Ding, Y. Yin, X. J. Yu, Y. C. Yuan, M. B. Perez, S. de Beer, G. J. Vancso, Y. L. Yu, S. Y. Zhang, *Eur. Polym. J.* **2020**, 134, 109845.

[7] a) R.-H. Jhang, C.-Y. Yang, M.-C. Shih, J.-Q. Ho, Y.-T. Tsai, C.-H. Chen, *J. Mater. Chem. A* **2018**, *6*, 17915; b) M. C. Shih, R. H. Jhang, Y. T. Tsai, C. W. Huang, Y. J. Hung, M. Y. Liao, J. Huang, C. H. Chen, *Small* **2019**, *15*, 1903363.

[8] Y. Jang, W. T. Choi, C. T. Johnson, A. J. Garcia, P. M. Singh, V. Breedveld, D. W. Hess, J. A. Champion, *ACS Biomater. Sci. Eng.* **2018**, *4*, 90.

[9] G. Panzner, B. Egert, H. P. Schmidt, *Surf. Sci.* **1985**, *151*, 400.

[10] a) J. Y. Kim, D. H. Youn, K. Kang, J. S. Lee, *Angew Chem Int Edit* **2016**, *55*, 10854; b) W. D. Chemelewski, H. C. Lee, J. F. Lin, A. J. Bard, C. B. Mullins, *J. Am. Chem. Soc.* **2014**, *136*, 2843.

[11] C. O. A. Olsson, D. Landolt, *Electrochim. Acta* **2003**, *48*, 1093.

[12] S. H. Yan, K. P. Abhilash, L. Y. Tang, M. Yang, Y. F. Ma, Q. Y. Xia, Q. B. Guo, H. Xia, *Small* **2019**, *15*, 1804371.

[13] M. Hans, A. Erbe, S. Mathews, Y. Chen, M. Solioz, F. Mucklich, *Langmuir* **2013**, *29*, 16160.

[14] E. C. Njagi, C. H. Chen, H. Genuino, H. Galindo, H. Huang, S. L. Suib, *Appl. Catal., B* **2010**, *99*, 103.

[15] a) O. Giraldo, S. L. Brock, W. S. Willis, M. Marquez, S. L. Suib, S. Ching, *J. Am. Chem. Soc.* **2000**, *122*, 9330; b) H. P. Zhang, F. F. Xu, J. Y. Xue, S. Y. Chen, J. J. Wang, Y. J. Yang, *Sci Rep-Uk* **2020**, 10, 6067; c) C. I. Lee, W. F. Yang, C. I. Hsieh, *J. Hazard. Mater.* **2004**, *114*, 45.

[16] Z. G. Dan, H. W. Ni, B. F. Xu, J. Xiong, P. Y. Xiong, *Thin Solid Films* **2005**, *492*, 93.

